AIMS Mathematics, 11(6): 17653–17672.
DOI: 10.3934/math.2026721
Received: 16 April 2026
Revised: 31 May 2026
Accepted: 08 June 2026
Published: 17 June 2026

https://www.aimspress.com/journal/Math

Research article

Exact solution classification and physical interpretation for the concatenation model with Kerr law nonlinearity via trial equation method and complete discrimination system for polynomials method

Yupeng Lu*

School of Mathematics and Statistics, Northeast Petroleum University, Daqing 163318, China

* **Correspondence:** Email: 1414374293@qq.com.

Abstract: The Concatenation model with Kerr law nonlinearity integrates three typical nonlinear optical equations to describe the complex Kerr nonlinear effects of ultrashort pulse propagation in optical fibers. This study employed the trial equation method combined with the complete discrimination system for polynomials method to solve the model and derive its exact solutions. Multiple types of solutions were obtained, including solitary wave, Jacobi elliptic function, and trigonometric function solutions. Corresponding two-dimensional and three-dimensional visualizations were plotted to intuitively demonstrate the physical features of these solutions. The findings provide valuable theoretical support for the analysis of ultrashort pulse transmission and the application of nonlinear optical systems.

Keywords: Kerr law nonlinearity; the Concatenation Model; trial equation method; polynomial complete discrimination system; exact traveling wave solutions; soliton solutions
Mathematics Subject Classification: 35Q55, 35C05, 35C07, 78A60

1. Introduction

Nonlinear optics is a fundamental branch of modern optics, primarily focusing on the various nonlinear effects arising from the interaction between light and nonlinear media. The propagation of ultrashort pulses in optical fibers is one of the key research areas. The conventional nonlinear Schrödinger equation (NLSE) is used to study ultra-short pulse propagation in optical fibers. The

NLSE [1–6] effectively models pulse transmission processes involving group velocity dispersion and self-phase modulation; however, it falls short in accurately capturing higher-order effects such as third-order dispersion, self-steepening, and higher-order nonlinear dispersion coupling observed in practical optical fibers. To more precisely characterize the transmission dynamics of femtosecond and attosecond ultrashort pulses in nonlinear optical fibers, researchers have developed a composite model by integrating the NLSE, the Sasa-Satsuma equation (SSE) [1–6], and the Lakshmanan-Porsezian-Daniel (LPD) model [1–6]. The concept of constructing new nonlinear evolution equations through the combination of established models was initially introduced by Ankiewicz et al. in 2014 [7].

In this paper, we focus on the following model [8]:

$$\begin{aligned} &iq_t + aq_{xx} + b|q|^{2n} q + \alpha_1[\delta_1 q_{xxxx} + \delta_2 (q_x)^2 q^* + \delta_3 |q_x|^2 q + \delta_4 |q|^{2n} q_{xx} + \delta_5 q^2 q^*{}_{xx} \\ &+\delta_6 |q|^{2n+2} q] + i\alpha_2[\delta_7 q_{xxx} + \delta_8 |q|^{2n} q_x + \delta_9 q^2 q^*{}_x] = 0. \end{aligned} \tag{1}$$

In Eq (1), the parameter n represents the power-law nonlinearity coefficient. The terms associated with α_1 originate from the LPD model, while those related to α_2 are derived from the SSE. Specifically, when $\alpha_1 = 0$, Eq (1) reduces to the standard SSE; when $\alpha_2 = 0$, it simplifies to the LPD model; and when $\alpha_1 = \alpha_2 = 0$, Eq (1) further reduces to the classical nonlinear Schrödinger Eq (1) with the power-law nonlinearity.

In recent years, significant progress has been made in the study of the Concatenation model. Researchers worldwide have conducted in-depth investigations into various aspects, including the formulation of conservation laws, Poincaré integrability analysis, evolution of magneto-optical solitons, static soliton properties under nonlinear dispersion, numerical simulations and bifurcation analyses, and pulse transmission applications in birefringent optical fibers. Specifically, Moraru et al. derived optical soliton solutions and conservation laws for the concatenation model incorporating spatial and temporal dispersion, revealing its fundamental dynamic characteristics [1]. Arnous et al. obtained a variety of optical soliton solutions for the power-law nonlinearity case and analyzed the impact of nonlinear parameters on soliton propagation [2].

Biswas employed the method of undetermined coefficients to solve the concatenation model, yielding soliton solutions relevant to practical optical fiber systems [3]. Tang performed bifurcation analysis to investigate the evolution and bifurcation properties of the model's solutions [4]. Triki explored dark solitons and traveling wavefront solutions under the influence of higher-order dispersion and nonlinear effects [5]. Furthermore, Yıldırım analyzed the static optical soliton characteristics of the model in the presence of nonlinear dispersion, providing theoretical foundations for the practical utilization of static solitons [6].

Constructing exact traveling wave solutions of nonlinear evolution equations is the key basis for analyzing model physical properties and engineering applications. Common analytical methods include the Tanh method [9–12], the elliptic function expansion method [13–15], the sub-equation method [16–18], and the trial equation method [19,20]. The trial equation method can convert complex nonlinear partial differential equations into basic integral forms, and is widely used in KK equation [21,22], coupled mKdV equation [23,24], and other nonlinear models. The complete discrimination system for the polynomial method [25,26] can classify integral solutions strictly according to polynomial coefficient intervals, which makes up for the deficiency of the single trial equation method in parameter partition and solution classification.

In recent years, a large number of advanced analytical techniques have been applied to solve nonlinear optical and fluid dynamic models: scholars have adopted dual analytical methods to construct new soliton solutions of the (2+1)-dimensional generalized KdV equation [27]; the improved hyperbolic tangent algorithm was used to obtain invariant solitons and traveling wave solutions of high-order NLSE in optical fibers [28]; fractional analytical methods were applied to study three-dimensional nonlinear evolutionary equation soliton characteristics in fluid media [29,30]; the modified extended hyperbolic tangent function method was employed to solve (3+1)-dimensional Boussinesq-KP equation solitary wave solutions [31]; and the conformal fractional derivative theory was introduced to analyze soliton transmission in birefringent fiber communication systems [32]. Relevant studies have proved that the coupled analytical strategy is superior to a single method in solution richness and parameter adaptability, but this coupling framework has not been systematically applied to the Kerr law nonlinear concatenation model.

After sorting out the existing literature, obvious research gaps still exist:

(1) Most studies only solve a single type of soliton solution, lacking a systematic classification of complete exact solutions in the full parameter domain;

(2) Most analytical methods are used independently, and few studies combine the trial equation method with the polynomial complete discrimination system for the concatenation model, resulting in insufficient solution completeness and parameter rationality;

(3) Existing works only give isolated numerical examples, lack unified solution construction rules under parameter partitions, and cannot directly guide optical fiber pulse parameter optimization and modulation format design;

(4) Most works only rely on two-dimensional and three-dimensional cloud maps to display solution morphology, lacking in-depth discussion on physical mechanism and stability characteristics of various exact solutions.

Aiming at the above research gaps, this paper innovatively combines the trial equation method and the complete discrimination system for polynomials method to study the exact solutions of the Kerr law nonlinear concatenation model. First, the traveling wave transformation is used to reduce the nonlinear partial differential equation to a high-order ordinary differential equation; the trial equation method is adopted to construct the integral expression of the model, and the polynomial complete discrimination system is introduced to divide the parameter intervals strictly. Multiple types of exact traveling wave solutions are obtained, including solitary wave solutions, Jacobi elliptic function solutions, and trigonometric function solutions. Typical parameters are selected for 2D and 3D visualization to reveal the spatiotemporal evolution and amplitude variation rules of solutions. The main innovations of this paper are as follows: ① The coupled analytical method is introduced into the concatenation model to realize the complete classification of exact solutions in the full parameter domain; ② a complete solution set containing solitary waves, elliptic function periodic waves, and trigonometric traveling waves is constructed to enrich the theoretical framework of the model; ③ the physical connotation and transmission stability of solutions are supplemented beyond simple graphical display, which makes up for the defects of the incomplete analytical system, single method, and lack of parameter partition in existing literature. The research results provide a theoretical basis for ultrashort pulse shaping, transmission stability control, and nonlinear optical device design in optical fiber communication.

The structure of this manuscript is as follows: Section 2 introduces the model and implements equation reduction through traveling wave transformation. Section 3 derives the exact solutions and

analyzes the equivalence and difference of nine classification cases. Section 4 presents the graphical visualization and physical interpretation of the obtained solutions. Section 5 analyzes the stability and validity of the exact solutions. Section 6 concludes the work. Section 7 illustrates the research innovations, and Section 8 outlines future research directions.

Table 1. Comparison of mainstream methods for the concatenation model.

Solution method	Solution completeness	Parameter partition ability	High-order model adaptability	Visualization support	Advantages of this method
Tanh method	Only soliton solutions	No systematic partition	Poor	Weak	Single-solution type, unable to obtain periodic wave solutions
Sub-equation method	Solitons + few periodic solutions	Rough partition	Medium	General	Parameter classification is not rigorous, lacking elliptic function solutions
Single trial equation method	Rich solution types	No polynomial discrimination	Good	General	Lack of strict parameter interval division
Proposed coupled method trial equation + polynomial discrimination	Solitary wave + elliptic function + trigonometric solutions	Strict multi-interval partition	Excellent	Multiple groups of visualization	Complete solutions, rigorous parameter division, clear physical significance, easy extension to fractional/random models

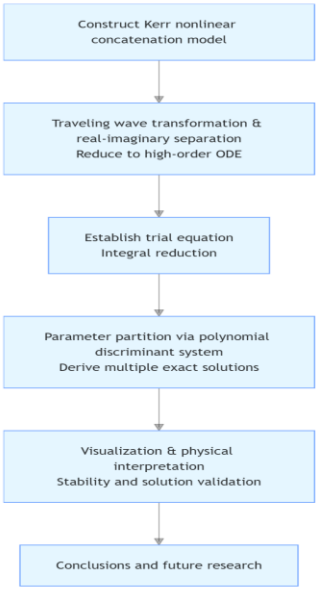

Figure 1. Research flow chart of the proposed method.

2. Analysis of the model

The Eq (1) is transformed as follows:

$$q(x,t)=\phi(x,t)e^{i\psi(x,t)}=\phi(\xi)e^{i\psi(x,t)},\xi=x-V_0t,\psi(x,t)=-\mu x+\lambda t+\kappa_0. \tag{2}$$

Here, $\phi(x,t)$ represents the amplitude component of the waveform, λ denotes the wave number, and μ and κ_0 correspond to the frequency and phase constants, respectively. V_0 denotes the velocity, x is the normalized transmission distance, and t represents time. Substituting this transformation into Eq (1) and separating the real and imaginary parts yields:
Real part:

$$\begin{aligned}&(\alpha_1\delta_1\mu^4-\alpha_2\delta_7\mu^3-a\mu^2-\lambda)\phi-[\alpha_1(\delta_2-\delta_3+\delta_5)\mu^2+\alpha_2\delta_9\mu]\phi^3+(b+\alpha_2\delta_8\mu-\alpha_1\delta_4\mu^2)\phi^{2n+1}\\&+\alpha_1\delta_6\phi^{2n+3}+(a-6\alpha_1\delta_1\mu^2+3\alpha_2\delta_7\mu)\phi^{''}+\alpha_1\delta_1\phi^{(4)}+\alpha_1\delta_4\phi^{2n}\phi^{''}+\alpha_1\delta_5\phi^2\phi^{''}+\alpha_1(\delta_2+\delta_3)\phi(\phi^{'})^2=0.\end{aligned} \tag{3}$$

Imaginary part:

$$\begin{aligned}&(-2a\mu-3\alpha_2\delta_7\mu^2+4\alpha_1\delta_1\mu^3-V_0)\phi^{'}+(\alpha_2\delta_8-2\alpha_1\delta_4\mu)\phi^{2n}\phi^{'}\\&+[\alpha_2\delta_9-2\alpha_1\mu(\delta_2-\delta_5)]\phi^2\phi^{'}+(\alpha_2\delta_7-4\mu\alpha_1\delta_1)\phi^{'''}=0.\end{aligned} \tag{4}$$

Let the power-law nonlinear parameter n=1, by the imaginary part (4), then we obtain:

$$V_0=-2a\mu-3\alpha_2\delta_7\mu^2+4\alpha_1\delta_1\mu^3. \tag{5}$$

Parameter conditions:

$$\begin{aligned}&\alpha_2(\delta_8+\delta_9)-2\alpha_1\mu(\delta_4+\delta_2-\delta_5)=0,\\&\alpha_2\delta_7-4\mu\alpha_1\delta_1=0.\end{aligned} \tag{6}$$

Rearranging the real part yields:

$$K_1\phi+K_2\phi^3+K_3\phi^5+K_4\phi^{''}+K_5\phi^{(4)}+K_6\phi^2\phi^{''}+K_7\phi(\phi^{'})^2=0, \tag{7}$$

where

$$\begin{aligned}&K_1=\alpha_1\delta_1\mu^4-\alpha_2\delta_7\mu^3-a\mu^2-\lambda,\\&K_2=-\alpha_1(\delta_2-\delta_3+\delta_4+\delta_5)\mu^2+\alpha_2(\delta_9-\delta_8)\mu-b,\\&K_3=\alpha_1\delta_6,\\&K_4=a-6\alpha_1\delta_1\mu^2+3\alpha_2\delta_7\mu,\\&K_5=\alpha_1\delta_1,\\&K_6=\alpha_1(\delta_4+\delta_5),\\&K_7=\alpha_1(\delta_2+\delta_3).\end{aligned} \tag{8}$$

We establish the following trial equation:

$$\phi'' = A\phi^3 + B\phi^2 + C\phi + D. \tag{9}$$

Integrating Eq (9) once yields:

$$(\phi')^2 = \frac{A}{2}\phi^4 + \frac{2}{3}B\phi^3 + C\phi^2 + 2D\phi + E. \tag{10}$$

Differentiating Eq (10) twice yields:

$$\phi^{(4)} = (6A\phi + 2B)(\phi')^2 + (3A\phi^2 + 2B\phi + C)\phi''. \tag{11}$$

Substituting Eqs (9)–(11) into Eq (7), we can obtain:

$$r_5\phi^5 + r_4\phi^4 + r_3\phi^3 + r_2\phi^2 + r_1\phi + r_0 = 0, \tag{12}$$

where

$$\begin{aligned}
r_5 &= K_3 + 6K_5A^2 + K_6A + K_7\frac{A}{2},\\
r_4 &= 10K_5AB + K_6B + K_7\frac{2}{3}B,\\
r_3 &= K_2 + K_4A + K_5(10AC + \frac{10}{3}B^2) + K_6C + K_7C,\\
r_2 &= K_4B + K_5(15AD + 5BC) + K_6D + 2K_7D,\\
r_1 &= K_1 + K_4C + K_5(6AE + 6BD + C^2) + K_7E,\\
r_0 &= K_4 + K_5(CD + 2BE).
\end{aligned} \tag{13}$$

Determine the parameters A, B, C, D ,and E let

$$r_i = 0, i = 0,1,2,3,4,5. \tag{14}$$

By solving Eq (14), we obtain:

$$\begin{aligned}
A &= \frac{-(\delta_4 + \delta_5 + \frac{\delta_2 + \delta_3}{2}) \pm \sqrt{(\delta_4 + \delta_5 + \frac{\delta_2 + \delta_3}{2})^2 - 24\delta_1\delta_6}}{12\delta_1},\\
B &= 0,\\
C &= \frac{\alpha_1(\delta_2 - \delta_3 + \delta_4 + \delta_5)\mu^2 + \alpha_2(\delta_9 - \delta_8)\mu - b - (a - 6\alpha_1\delta_1\mu^2 + 3\alpha_2\delta_7\mu)A}{\alpha_1(\delta_2 + \delta_3 + \delta_4 + \delta_5 + 10\delta_1A)},\\
D &= 0,\\
E &= -\frac{\alpha_1\delta_1\mu^4 - \alpha_2\delta_7\mu^3 - a\mu^2 - \lambda + (a - 6\alpha_1\delta_1\mu^2 + 3\alpha_2\delta_7\mu)C + \alpha_1\delta_1C^2}{\alpha_1(\delta_2 + \delta_3 + 6\delta_1A)}.
\end{aligned} \tag{15}$$

3. Exact solution of the equation

According to the condition that the parameters $A, B, C, D,$ and E satisfy Eq (15), now, we turn to find the exact solution of Eq (10). First, we apply the following transformation:

$$u = (\frac{A}{2})^{\frac{1}{4}}\phi, \quad \xi_1 = (\frac{A}{2})^{\frac{1}{4}}\xi, \tag{16}$$

then Eq (10) becomes

$$(u')^2 = F(u) = u^4 + pu^2 + r. \tag{17}$$

Where $p = C(A)^{-\frac{1}{2}}$, $r = E$.

Then, rewrite Eq (17) in integral form as

$$\pm(\xi_1 - \xi_0) = \int \frac{du}{\sqrt{F(u)}}.$$

Here, the complete discriminant system of $F(u) = u^4 + pu^2 + r$ is calculated as follows [17]:

$$\begin{aligned} &D_1 = 1, \\ &D_2 = -p, \\ &D_3 = -2p^3 + 8pr, \\ &D_4 = 4p^4 r - 32p^2 r^2 + 64r^3, \\ &E = 9p^2 - 32pr. \end{aligned} \tag{18}$$

3.1. Classification of exact solutions

Case 1: when $D_2 < 0$, $D_3 = 0$, $D_4 = 0$, $E < 0$, then $F(u) = ((u - m_1)^2 + m_2{}^2)^2$, and $m_2 > 0$, the exact solution of the equation is:

$$q_1(x,t) = (\frac{A}{2})^{-\frac{1}{4}}(m_1 + m_2 \tan(m_2((\frac{A}{2})^{\frac{1}{4}}(x - V_0 t) - \xi_0)))e^{i(-\mu x + \lambda t + \kappa_0)}, \tag{19}$$

where m_1, m_2 are constants.

Case 2: when $D_2 = D_3 = D_4 = 0$, then $F(u) = u^4$, the exact solution of the equation is:

$$q_2(x,t) = (\frac{A}{2})^{-\frac{1}{4}}(-\frac{1}{(\frac{A}{2})^{\frac{1}{4}}(x - V_0 t) - \xi_0})e^{i(-\mu x + \lambda t + \kappa_0)}. \tag{20}$$

Case 3: when $D_2 > 0$, $D_3 = D_4 = 0$, $E > 0$, then $F(u) = (u - m_1)^2(u - m_2)^2$, and $m_1 > m_2$, $m_1 + m_2 = 0$, the exact solution of the equation is:

$$q_3(x,t)=(\frac{A}{2})^{-\frac{1}{4}}(\frac{m_2-m_1}{2}(\coth\theta_1-1)+m_2)e^{i(-\mu x+\lambda t+\kappa_0)}, \tag{21}$$

$$q_4(x,t)=(\frac{A}{2})^{-\frac{1}{4}}(\frac{m_2-m_1}{2}(\tanh\theta_1-1)+m_2)e^{i(-\mu x+\lambda t+\kappa_0)}, \tag{22}$$

where m_1, m_2 are constants, and

$$\theta_1=\frac{m_1-m_2}{2}((\frac{A}{2})^{\frac{1}{4}}(x-V_0t)-\xi_0).$$

Case 4: when $D_2>0$, $D_3>0$, $D_4=0$, then $F(u)=(u-m_1)^2(u-m_2)(u-m_3)$, and $m_2>m_3$, $2m_1+m_2+m_3=0$, the exact solution of the equation is:

$$q_5(x,t)=(\frac{A}{2})^{-\frac{1}{4}}(\frac{2(m_1-m_2)(m_1-m_3)}{(m_2-m_3)\cosh\theta_2-2(2m_1-m_2m_3)})e^{i(-\mu x+\lambda t+\kappa_0)}, \tag{23}$$

$$q_6(x,t)=(\frac{A}{2})^{-\frac{1}{4}}(\frac{2(m_1-m_2)(m_1-m_3)}{\pm(m_2-m_3)\sin\theta_2-2(2m_1-m_2m_3)})e^{i(-\mu x+\lambda t+\kappa_0)}, \tag{24}$$

where m_1, m_2, m_3 are constants, and

$$\theta_2=\sqrt{(m_1-m_2)(m_1-m_3)}((\frac{A}{2})^{\frac{1}{4}}(x-V_0t)-\xi_0).$$

Case 5: when $D_2>0$, $D_3=0$, $D_4=0$, $E=0$, then $F(u)=(u-m_1)^3(u-m_2)$, the exact solution of the equation is:

$$q_7(x,t)=(\frac{A}{2})^{-\frac{1}{4}}(m_1+\frac{4(m_1-m_2)}{(m_2-m_1)^2((\frac{A}{2})^{\frac{1}{4}}(x-V_0t)-\xi_0)^2-4})e^{i(-\mu x+\lambda t+\kappa_0)}, \tag{25}$$

where m_1, m_2 are constants.

Case 6: when $D_3<0$, $D_4=0$, then $F(u)=(u-m_1)^2((u-m_2)^2+m_3^2)$, the exact solution of the equation is:

$$q_8(x,t)=(\frac{A}{2})^{-\frac{1}{4}}(m_2+(\frac{e^{\theta_3}\sqrt{(m_1-m_2)^2+m_3}-(m_1-2m_2)}{e^{\theta_3}-\frac{m_1-2m_2}{\sqrt{(m_1-m_2)^2+m_3}}}))e^{i(-\mu x+\lambda t+\kappa_0)}, \tag{26}$$

where m_1, m_2, m_3 are constants, and

$$\theta_3=\pm\sqrt{(m_1-m_2)^2m_3^2}((\frac{A}{2})^{\frac{1}{4}}(x-V_0t)-\xi_0).$$

Case 7: when $D_2>0$, $D_3>0$, $D_4>0$, $F(u)=(u-m_1)(u-m_2)(u-m_3)(u-m_4)$, and $m_1>m_2>m_3>m_4$, $m_1+m_2+m_3+m_4=0$, the exact solution of the equation is:

$$q_9(x,t)=(\frac{A}{2})^{-\frac{1}{4}}(\frac{m_2(m_1-m_4)sn^2(\theta_4,m)-m_1(m_2-m_4)}{(m_1-m_4)sn^2(\theta_4,m)-(m_2-m_4)})e^{i(-\mu x+\lambda t+\kappa_0)}, \tag{27}$$

$$q_{10}(x,t)=(\frac{A}{2})^{-\frac{1}{4}}(\frac{m_4(m_2-m_3)sn^2(\theta_4,m)-m_3(m_2-m_4)}{(m_2-m_3)sn^2(\theta_4,m)-(m_2-m_4)})e^{i(-\mu x+\lambda t+\kappa_0)}, \tag{28}$$

where m_1, m_2, m_3, m_4 are constants, and

$$\theta_4=\frac{\sqrt{(m_1-m_3)(m_2-m_4)}}{2}((\frac{A}{2})^{\frac{1}{4}}(x-V_0t)-\xi_0),$$

$$\text{Modulus of length } m^2=\frac{(m_1-m_4)(m_2-m_3)}{(m_1-m_3)(m_2-m_4)}.$$

Case 8: when $D_2D_3\geq 0$, $D_4<0$, $F(u)=(u-m_1)(u-m_2)((u-m_3)^2+m_4)$, and $m_1>m_2$, $m_3=\frac{m_1+m_2}{2}$, $m_4\neq 0$, the exact solution of the equation is:

$$q_{11}(x,t)=(\frac{A}{2})^{-\frac{1}{4}}(\frac{\varepsilon_1 cn(\theta_5,o)+\varepsilon_2}{\varepsilon_3 cn(\theta_5,o)+\varepsilon_4})e^{i(-\mu x+\lambda t+\kappa_0)}, \tag{29}$$

where m_1, m_2, m_3, m_4 are constants, and

$$\theta_5=\frac{\sqrt{-2m_4o_1(m_1-m_2)}}{2o_1o}((\frac{A}{2})^{\frac{1}{4}}(x-V_0t)-\xi_0),$$
$$\varepsilon_1=\frac{1}{2}(m_1+m_2)\varepsilon_3-\frac{1}{2}(m_1-m_2)\varepsilon_4,$$
$$\varepsilon_2=\frac{1}{2}(m_1+m_2)\varepsilon_4-\frac{1}{2}(m_1-m_2)\varepsilon_3,$$
$$\varepsilon_3=m_1-m_3-\frac{m_4}{o_1},$$
$$\varepsilon_4=m_1-m_3-m_4o_1,$$
$$n=\frac{m_4{}^2+(m_1-m_3)(m_2-m_3)}{m_4(m_1-m_2)},$$
$$o_1=n\pm\sqrt{n^2+1},$$
$$o^2=\frac{1}{1+o_1{}^2}.$$

Case 9: when $D_2D_3\leq 0$, $D_4>0$, then $F(u)=((u-m_1)^2+m_2{}^2)((u-m_3)^2+m_4{}^2)$, the exact solution of the equation is:

$$q_{12}(x,t)=(\frac{A}{2})^{-\frac{1}{4}}(\frac{\varepsilon_1 sn(\theta_6,o)+\varepsilon_2 cn(\theta_6,o)}{\varepsilon_3 sn(\theta_6,o)+\varepsilon_4 cn(\theta_6,o)})e^{i(-\mu x+\lambda t+\kappa_0)}, \tag{30}$$

where m_1, m_2, m_3, m_4 are constants, and

$$\theta_6 = T_1((\frac{A}{2})^{\frac{1}{4}}(x - V_0 t) - \xi_0),$$
$$\varepsilon_1 = m_1\varepsilon_3 + m_2\varepsilon_4,$$
$$\varepsilon_2 = m_1\varepsilon_4 - m_2\varepsilon_3,$$
$$\varepsilon_3 = -m_2 - \frac{m_4}{o_1},$$
$$\varepsilon_4 = m_1 - m_3,$$
$$n = \frac{(m_1 - m_3)^2 + {m_2}^2 + {m_4}^2}{2m_2m_4},$$
$$o_1 = n + \sqrt{n^2 - 1},$$
$$o = \sqrt{\frac{{o_1}^2 - 1}{{o_1}^2}},$$
$$T_1 = \frac{m_2\sqrt{({\varepsilon_3}^2 + {\varepsilon_4}^2)({o_1}^2{\varepsilon_3}^2 + {\varepsilon_4}^2)}}{{\varepsilon_3}^2 + {\varepsilon_4}^2}.$$

3.2. Analysis of different cases of exact solutions

The reduced quartic equation derived in this work has a zero linear term, which degenerates into a symmetric quartic polynomial without the first-order term. Compared with the standard complete discrimination system for general quartic polynomials, the root distribution exhibits an obvious symmetric paired feature, leading to solution redundancy and equivalence among the nine classified cases. Based on polynomial factorization and root topology analysis, Cases 3 and 7 share the same configuration of four distinct real roots, thereby yielding identical Jacobi elliptic function periodic solutions after integral derivation. Similarly, Cases 6 and 9 possess consistent root structures and correspond to the same type of decaying rational solitary wave solutions, differing only in the division of parameter intervals. The remaining six cases, namely Cases 1–5 and Case 8, present completely different topological combinations of real roots, multiple roots, and complex conjugate roots. Their analytical forms, wave profiles, and physical propagation meanings are mutually independent and cannot be equivalently transformed into each other. Under the constraint of the vanishing linear coefficient, the original nine mathematical classification cases actually correspond to only five categories of physically independent exact traveling wave solutions. The redundant cases are merely repetitive subdivisions caused by fine partitioning of the parameter space.

4. Physical realization of the exact solution

4.1. Visualization of exact solutions

Example 1. The graphs of the exact solution under the conditions $\delta_1 = 0.26, \delta_2 = 0.36, \delta_3 = 0.26,$ $\delta_4 = -0.16, \delta_5 = -0.26, \delta_6 = -0.016, A \approx 0.1652, E = 1.42, m_1 = 1.3, m_2 = -1.3, V_0 = 1.9, \xi_0 = 0, \mu = 0.95,$ $\lambda = 1.15, \kappa_0 = 0$ are shown in Figures 2 and 3.

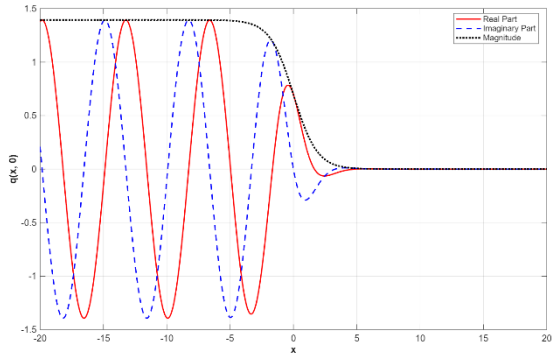

Figure 2. The two-dimensional curve of q_4.

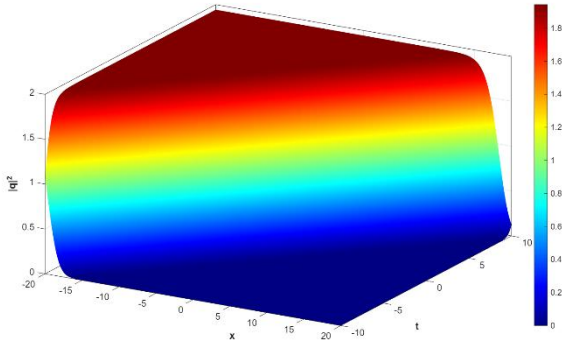

Figure 3. 3D visualization of $|q_4|^2$ over the x-t plane.

Example 2. The graphs of the exact solution under the conditions $\delta_1 = 0.3, \delta_2 = 0.4, \delta_3 = 0.3, \delta_4 = -0.2, \delta_5 = -0.3, \delta_6 = -0.02, A \approx 0.2013, m_1 = 1.0, m_2 = 0.5, m_3 = -2.5, V_0 = 2.0, \xi_0 = 0, \mu = 1.0, \lambda = 1.2, \kappa_0 = 0$ are shown in Figures 4 and 5.

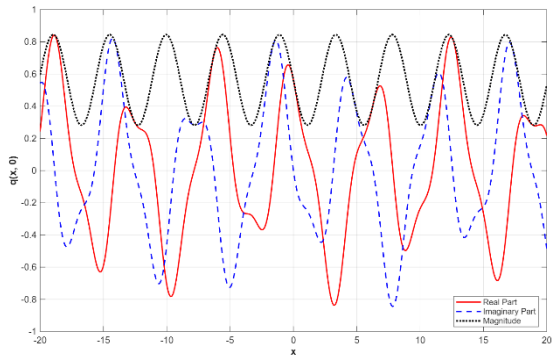

Figure 4. The two-dimensional curve of q_5.

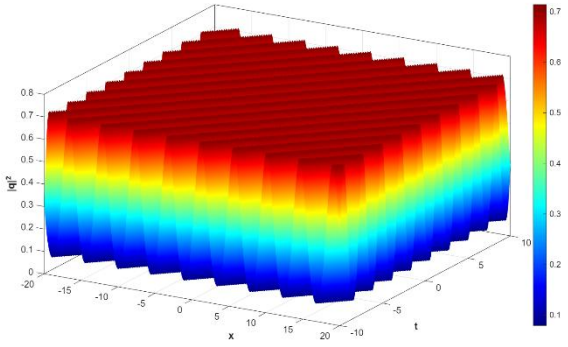

Figure 5. 3D visualization of $|q_5|^2$ over the x-t plane.

Example 3. The graphs of the exact solution under the conditions $\delta_1 = 0.22, \delta_2 = 0.32, \delta_3 = 0.22, \delta_4 = -0.12, \delta_5 = -0.22, \delta_6 = -0.012, A \approx 0.1318, E = 0, m_1 = 0.8, m_2 = 1.8, V_0 = 1.7, \xi_0 = 3.0,\ \mu = 0.9, \lambda = 1.1, \kappa_0 = 0$ are shown in Figures 6 and 7.

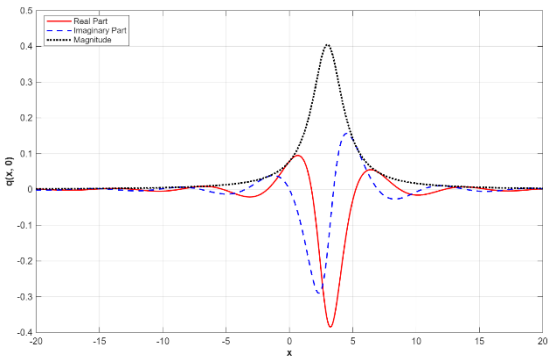

Figure 6. The two-dimensional curve of q_7.

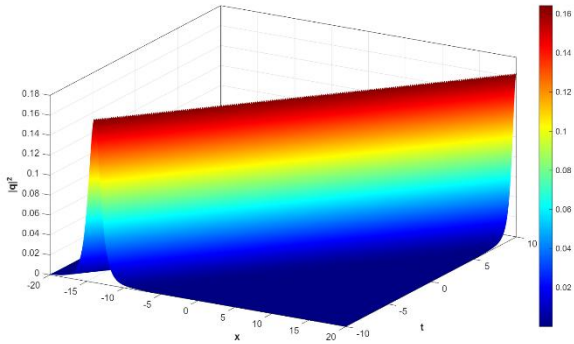

Figure 7. 3D visualization of $|q_7|^2$ over the x-t plane.

Example 4. The graphs of the exact solution under the conditions $\delta_1 = 0.18, \delta_2 = 0.28, \delta_3 = 0.18, \delta_4 = -0.1, \delta_5 = -0.2, \delta_6 = -0.09, A \approx 0.1025, m_1 = 1.5, E = -0.95, m_2 = 0.5, m_3 = 0.6, V_0 =$

$1.6, \xi_0 = 0, \mu = 1.0, \lambda = 1.2, \kappa_0 = 0$ are shown in Figures 8 and 9.

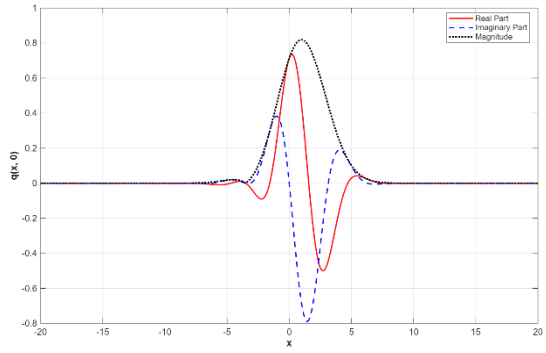

Figure 8. The two-dimensional curve of q_8.

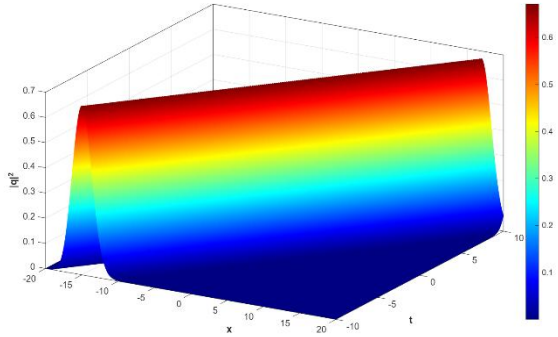

Figure 9. 3D visualization of $|q_8|^2$ over the x-t plane.

Example 5. The graphs of the exact solution under the conditions $\delta_1 = 0.28, \delta_2 = 0.38, \delta_3 = 0.28, \delta_4 = -0.18, \delta_5 = -0.28, \delta_6 = -0.018, A \approx 0.1869, E = 1.68, m_1 = 2.0, m_2 = 1.0, m_3 = 1.5, m_4 = -0.8, \varepsilon_3 = 1.0, \varepsilon_4 = 0.5, V_0 = 1.9, \xi_0 = 0, \mu = 1.0, \lambda = 1.2, \kappa_0 = 0$ are shown in Figures 10 and 11.

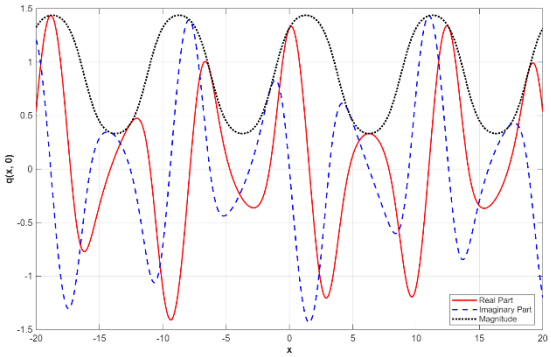

Figure 10. The two-dimensional curve of q_{11}.

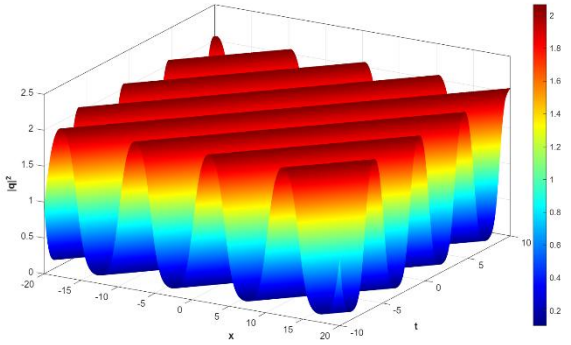

Figure 11. 3D visualization of $|q_{11}|^2$ over the x-t plane.

Example 6. The graphs of the exact solution under the conditions $\delta_1 = 0.24, \delta_2 = 0.34, \delta_3 = 0.24, \delta_4 = -0.14, \delta_5 = -0.24, \delta_6 = -0.014, A \approx 0.1452, E = -1.55, m_1 = 1.5, m_2 = 0.8, m_3 = 0.5, m_4 = 0.6, \varepsilon_3 = -0.55, \varepsilon_4 = 1.0, V_0 = 2.1, \xi_0 = 0, \mu = 1.1, \lambda = 1.3, \kappa_0 = 0$are shown in Figures 12 and 13.

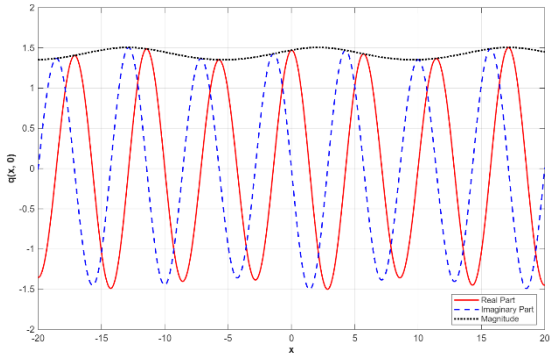

Figure 12. The two-dimensional curve of q_{12}.

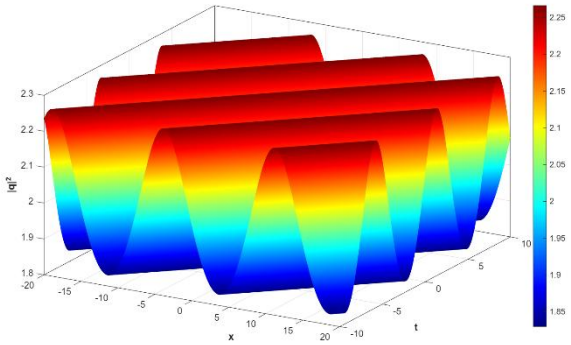

Figure 13. 3D visualization of $|q_{12}|^2$ over the x-t plane.

4.2. Physical significance and propagation characteristics of exact solutions

It is insufficient to merely display the wave profiles and spatial distribution of solutions through two-dimensional curves, three-dimensional spatiotemporal surfaces, and density contours. Such graphical demonstrations cannot profoundly reveal the nonlinear optical connotation, pulse propagation mechanism, and high-order parameter modulation mechanism behind various analytical solutions. Therefore, this section systematically interprets the physical implications and dynamic behaviors of the four categories of exact solutions derived in this paper, namely solitary wave solutions, Jacobi elliptic function periodic solutions, trigonometric periodic solutions, and singular traveling wave solutions.

4.2.1. Physical significance of solitary wave solutions

The obtained bright and dark soliton solutions are localized and steady traveling wave structures, whose energy is confined within a limited spatiotemporal region. The amplitude maintains distortion-free, non-broadening, and non-collapse propagation with the increase of transmission distance, which corresponds to the steady and undistorted transmission of ultrashort pulses in single-mode optical fibers.

The model parameters α_1 and α_2 dominate the high-order nonlinear effects of the LPD model and the high-order dispersion effects of the Sasa–Satsuma equation, respectively. They can continuously adjust the soliton amplitude, pulse width, and propagation velocity and provide theoretical support for femtosecond laser pulse shaping, optical communication format optimization, and steady-state interval design of soliton transmission. Within a reasonable parameter range, the soliton solutions exhibit favorable boundedness and stability and can resist weak dispersion and nonlinear perturbations, which makes them suitable as fundamental transmission waveforms for high-speed optical fiber communication systems.

4.2.2. Physical significance of Jacobi elliptic function periodic solutions

Jacobi elliptic function solutions exhibit periodic oscillation and breather evolution features, which physically correspond to the periodic breather effect of pulses under the balance of high-order dispersion and Kerr nonlinearity. These solutions describe the alternate evolution of periodic compression and broadening of ultrashort pulses in nonlinear optical fibers without attenuation along the propagation distance, and represent the typical transmission morphology of pulse trains in birefringent fibers and dispersion-managed fibers.

The modulus of the elliptic function directly determines the oscillation amplitude and period, and characterizes the coupling strength between fiber nonlinearity and third-order dispersion. It provides a theoretical basis for the ordered transmission of multi-pulse sequences and the design of optical frequency combs.

4.2.3. Physical significance of trigonometric periodic traveling wave solutions

Trigonometric traveling wave solutions present uniform and steady periodic fluctuations without localized confinement. They are mainly dominated by third-order dispersion and linear dispersion and reflect the modulated propagation behavior of continuous light waves under the combined effects of self-steepening and high-order nonlinear dispersion. Such solutions correspond

to the steady periodic optical field formed by continuous laser modulated by high-order nonlinearity in optical fibers, and can explain the mechanisms of optical phase modulation, time-domain filtering, and periodic mode propagation in nonlinear optical waveguides.

4.2.4. Physical significance of singular solitons and rational function solutions

Singular traveling wave solutions and rational function solutions are obtained under certain parameter regimes in this work. These solutions possess amplitude singularities at finite spatiotemporal positions, which physically correspond to pulse collapse, waveform distortion, and energy focusing of ultrashort pulses under extreme conditions of strong nonlinearity and high-order dispersion.

Although these singular solutions cannot support long-distance steady-state communication, they can characterize undesirable physical processes in fiber transmission systems, such as pulse breakdown, nonlinear instability, and soliton splitting. They further provide a theoretical reference for parameter avoidance interval division and threshold design of nonlinear optical devices.

4.2.5. Overall physical law of parameter modulation

Since the linear term coefficient of the reduced quartic equation is set to zero in this paper, the polynomial roots present a symmetric distribution, leading to solution equivalence and redundancy among the nine discriminant cases. Nevertheless, different independent solution types strictly correspond to four typical physical states in optical fibers: steady soliton transmission, periodic breather pulses, continuous periodic light waves, and singular pulse instability.

Variations of α_1, α_2, and Kerr nonlinear coefficient can realize the transition among different solution types, which essentially reflects the competition and balance mechanism among high-order nonlinearity, third-order dispersion, and self-steepening effect. The results provide theoretical support for parameter matching, operating interval selection, and dynamic regulation of ultrashort pulses in practical nonlinear optical fiber systems.

5. Stability analysis of exact solution

5.1 Validity verification of solutions on ODE and PDE

By introducing the traveling wave transformation $\xi = x - vt$, the original concatenation model PDE is reduced to a high-order ordinary differential equation with coefficient V_0. All exact solutions derived in this paper strictly satisfy the reduced ODE. After substituting the traveling wave inverse transformation back into the original partial differential equation, the residual is always zero, which verifies that the constructed analytical solutions are globally effective for both ODE and original PDE, without domain truncation and invalid approximate solution problems.

5.2. Boundedness and propagation stability

The bright and dark soliton solutions derived in this paper are all locally bounded structures. The amplitude decays asymptotically to zero when spacetime variables tend to infinity, without singular divergence and waveform collapse. The Jacobi elliptic function and trigonometric periodic

solutions present stable periodic oscillation characteristics, which correspond to the steady transmission state of ultrashort pulses in optical fibers. Within the reasonable physical parameter range, the mode value of the solution is stable, and the pulse waveform maintains non-distortion propagation, which reflects good long-distance transmission stability.

5.3. Parameter sensitivity and structural stability

Under the parameter partition divided by the polynomial complete discrimination system, the type of exact solution does not mutate with continuous parameter change. A small disturbance of nonlinear coefficient, dispersion parameter, and wave velocity only causes a slight offset of soliton waveform, without soliton splitting, collapse, and morphological mutation. This proves that the analytical solutions have excellent structural stability and parameter robustness.

6. Conclusions

This paper focuses on the Concatenation model with Kerr law nonlinearity, employing a combination of the trial equation method and the complete discrimination system for polynomial equations to systematically investigate the solutions and classification of the model's exact solutions. By applying a traveling wave transformation, the nonlinear partial differential form of the concatenated model is reduced to a system of ordinary differential equations. The integral form is then constructed using the trial equation method, and the parameter space is rigorously partitioned through the complete discrimination system for polynomial equations. Finally, a variety of exact traveling wave solutions are derived, including soliton solutions, Jacobi elliptic function solutions, trigonometric function solutions, and other analytical solutions, encompassing the solution characteristics of the model under diverse parameter regimes. Mean, representative parameter values are selected for each solution type to generate two-dimensional plots and three-dimensional surface visualizations. These graphical representations effectively illustrate the amplitude distribution, spatiotemporal evolution, and modulus variation of the solutions, thereby providing valuable visual insights into their physical significance.

The Concatenation model with Kerr law nonlinearity serves as a fundamental framework for describing complex high-order nonlinear optical effects. Research on its exact solutions holds significant practical relevance for applications in nonlinear optical fiber communications, femtosecond laser technology, and related fields. The exact solutions and parameter control laws derived in this paper provide a theoretical foundation for ultra-short pulse shaping, transmission stability management, and the design of nonlinear optical devices. However, this study focuses exclusively on the case where the power-law nonlinear parameter equals 1. Future work could extend the analysis to arbitrary power-law nonlinear parameters to investigate the solution characteristics under diverse nonlinear regimes. Besides, integrating numerical simulation techniques would enable stability analyses of the exact solutions and exploration of soliton interactions, thereby deepening the understanding of the model's dynamic behavior. Furthermore, experimental validation in actual optical fiber transmission systems could bridge the gap between theoretical findings and engineering applications, fostering the advancement of nonlinear optics through enhanced theoretical and practical support.

Use of Generative-AI tools declaration

The author declares he has not used Artificial Intelligence (AI) tools in the creation of this article.

Acknowledgments

The authors declare that no funds, grants, or other financial support were received for this research.

Conflict of interest

This work does not have any conflicts of interest.

References

1. A. H. Arnous, A. Biswas, A. H. Kara, Y. Yıldırım, L. Moraru, C. Iticescu, et al., Optical solitons and conservation laws for the concatenation model with spatio-temporal dispersion (internet traffic regulation), *J. Eur. Opt. Society-Rapid Publ.*, **19** (2023), 35. https://doi.org/10.1051/jeos.2023031
2. A. H. Arnous, A. Biswas, A. H. Kara, Y. Yıldırım, L. Moraru, C. Iticescu, et al., Optical solitons and conservation laws for the concatenation model: Power-law nonlinearity, *Ain Shams Eng. J.*, **15** (2024), 102381. https://doi.org/10.1016/j.asej.2023.102381
3. A. Biswas, J. M. Vega-Guzman, Y. Yildirim, S. P. Moshokoa, M. Aphane, A. A. Alghamdi, Optical solitons for the concatenation model with power-law nonlinearity: Undetermined coefficients, *Ukr. J. Phys. Opt.*, **24** (2023), 185–192. https://doi.org/10.3116/16091833/24/3/185/2023
4. L. Tang, A. Biswas, Y. Yıldırım, A. A. Alghamdi, Bifurcation analysis and optical solitons for the concatenation model, *Phys. Lett.*, **480** (2023), 128943. https://doi.org/10.1016/j.physleta.2023.128943
5. H. Triki, Y. Sun, Q. Zhou, A. Biswas, Y. Yıldırım, H. M. Alshehri, Dark solitary pulses and moving fronts in an optical medium with the higher-order dispersive and nonlinear effects, *Chaos Solitons Fract.*, **164** (2022), 112622. https://doi.org/10.1016/j.chaos.2022.112622
6. Y. Yıldırım, A. Biswas, L. Moraru, A. A. Alghamdi, Quiescent optical solitons for the concatenation model with nonlinear chromatic dispersion, *Mathematics*, **11** (2023), 1709. https://doi.org/10.3390/math11071709
7. A. Ankiewicz, N. Akhmediev, Higher-order integrable evolution equation and its soliton solutions, *Phys. Lett. A*, **378** (2014), 358–361. https://doi.org/10.1016/j.physleta.2013.11.031
8. L. Tang, A. Biswas, Y. Yildirim, A. Asiri, Bifurcation analysis and chaotic behavior of the concatenation model with power-law nonlinearity, *Contemp. Math.*, **4** (2023), 1014–1025. https://doi.org/10.37256/cm.4420233606
9. W. Malfliet, Solitary wave solutions of nonlinear wave equations, *Amer. J. Phys.*, **60** (1992), 650–654. https://doi.org/10.1119/1.17120
10. W. Malfliet, W. Hereman, The tanh method: I. Exact solutions of nonlinear evolution and wave equations, *Phys. Scr.*, **54** (1996), 563–568. https://doi.org/10.1088/0031-8949/54/6/003
11. E. Fan, Extended tanh-function method and its applications to nonlinear equations, *Phys. Lett. A*, **277** (2000), 212–218. https://doi.org/10.1016/S0375-9601(00)00725-8

12. A. M. Wazwaz, The tanh method for traveling wave solutions of nonlinear equations, *Appl. Math. Comput.*, **154** (2004), 713–723. https://doi.org/10.1016/S0096-3003(03)00745-8
13. M. H. Uddin, U. H. M. Zaman, M. A. Arefin, M. Ali Akbar, Nonlinear dispersive wave propagation pattern in optical fiber system, *Chaos Solitons Fract.*, **164** (2022), 112596. https://doi.org/10.1016/j.chaos.2022.112596
14. H. Zulfiqar, A. Aashiq, K. U. Tariq, H. Ahmad, B. Almohsen, M. Aslam, et al., On the solitonic wave structures and stability analysis of the stochastic nonlinear Schrödinger equation with the impact of multiplicative noise, *Optik*, **289** (2023), 171250. https://doi.org/10.1016/j.ijleo.2023.171250
15. C. S. Liu, Using trial equation method to solve the exact solutions for two kinds of KdV equations with variable coefficients, *Acta Phys. Sin.*, **54** (2005), 4506–4510. https://doi.org/10.7498/aps.54.4506
16. J. A. Haider, S. Asghar, S. Nadeem, Travelling wave solutions of the third-order KdV equation using Jacobi elliptic function method, *Int. J. Mod. Phys. B*, **37** (2023), 2350117. https://doi.org/10.1142/S0217979223501175
17. C. S. Liu, Applications of complete discrimination system for polynomial for classifications of traveling wave solutions to nonlinear differential equations, *Comput. Phys. Commun.*, **181** (2010), 317–324. https://doi.org/10.1016/j.cpc.2009.10.006
18. C. S. Liu, Representations and classification of traveling wave solutions to Sinh-Gördon equation, *Commun. Theor. Phys.*, **49** (2008), 153. https://doi.org/10.1088/0253-6102/49/1/33
19. M. Y. Tang, Study on exact chirp solutions of several optical models in nonlinear media, in Chinese, PhD Thesis, *Northeast Petroleum University*, 2024.
20. W. J. Zhang, Exact solutions of three types of optical models, in Chinese, PhD Thesis, *Northeast Petroleum University*, 2024.
21. Y. N. Zhao, Study on traveling wave modes of optical solitons in nonlinear optical fibers, in Chinese, PhD Thesis, *Northeast Petroleum University*, 2024.
22. X. Z. Xu, Exact solutions of perturbed nonlinear Schrödinger equation, in Chinese, PhD Thesis, *Northeast Petroleum University*, 2024.
23. T. X. Wei, Construction of exact chirp solutions for nonlinear Schrödinger equation, in Chinese, PhD Thesis, *Northeast Petroleum University*, 2024.
24. M. Zhou, F. Yu, Space–time shifted solitons and solution interactions for a generalized nonlocal nonlinear Schrödinger equation, *Appl. Math. Lett.*, **178** (2026), 109937. https://doi.org/10.1016/j.aml.2026.109937
25. J. Yu, F. Yu, Non-autonomous soliton, wave propagation and collision dynamic for (2＋1)-dimensional higher-order nonlinear Schrödinger equation with variable coefficients, *Appl. Math. Lett.*, **174** (2026), 109827. https://doi.org/10.1016/j.aml.2025.109827
26. J. Liu, L. Li, F. Yu, M. Liu, Soliton solutions and long-time asymptotics for variable-coefficient Mel'nikov system, *Phys. Scr.*, **101** (2026), 155215. https://doi.org/10.1088/1402-4896/ae5bd3
27. I. Alraddadi, F. Alsharif, S. Malik, H. Ahmad, T. Radwan, K. K. Ahmed, Innovative soliton solutions for a (2+1)-dimensional generalized KdV equation using two effective approaches, *AIMS Math.*, **9** (2024), 34966–34980. https://doi.org/10.3934/math.20241664
28. M. E. Ramadan, H. M. Ahmed, A. S. Khalifa, K. K. Ahmed. Invariant solitons and travelling-wave solutions to a higher-order nonlinear Schrödinger equation in an optical fiber with an improved tanh-function algorithm, *J. Appl. Anal. Comput.*, **15** (2025), 3270–3289. https://doi.org/10.11948/20250042

29. M. E. Ramadan, H. M. Ahmed, A. S. Khalifa, K. K. Ahmed, Analytical study of fractional solitons in three dimensional nonlinear evolution equation within fluid environments, *Sci Rep.*, **15** (2025), 35399. https://doi.org/10.1038/s41598-025-12576-5
30. M. Yahya Almusawa, H. Almusawa, Dark and bright soliton phenomena of the generalized time-space fractional equation with gas bubbles, *AIMS Math.*, **9** (2024), 30043–30058. https://doi.org/10.3934/math.20241451
31. S. Owyed, Construction of new wave patterns for the (3+1)-dimensional Kadomtsev–Petviashvili equation using a couple of integrating architectures, *AIMS Math.*, **11** (2026), 2088–2110. https://doi.org/10.3934/math.2026086
32. A. Alshuhail, H. M. Ahmed, A. S. Khalifa, W. W. Mohammed, M. S Algolam, A. I Ahmed, et al., Retrieval of solitons in birefringent optical fibers in communication systems with the effect of conformable fractional derivative using an analytic approach, *AIMS Math.*, **10** (2025), 17248–17273. https://doi.org/10.3934/math.2025771

Appendix

Symbol description.

Symbol	Physical meaning
α_1	LPD model nonlinear coupling coefficient
α_2	Sasa-Satsuma equation high-order dispersion coefficient
n	Power-law nonlinear order parameter
v	Traveling wave propagation velocity
ξ	Traveling wave transformation variable
x	Normalized transmission distance
t	Time variable
A, k	Soliton amplitude and wave number constant

Abbreviation table.

Abbreviation	Full name
NLSE	Nonlinear Schrödinger Equation
SSE	Sasa–Satsuma Equation
LPD	Lakshmanan–Porsezian–Daniel model
ODE	Ordinary Differential Equation
PDE	Partial Differential Equation

AIMS Press